Structure and Reactivity of a_n and a_n* Peptide Fragments Investigated Using Isotope Labeling, Tandem Mass Spectrometry, and Density Functional Theory Calculations*

Benjamin J. Bythell,[b] Samuel Molesworth,[a] Sandra Osburn,[a] Travis Cooper,[a] Béla Paizs,[b] and Michael Van Stipdonk[a]

[a] Department of Chemistry, Wichita State University, Wichita, Kansas, USA
[b] Department of Molecular Biophysics, German Cancer Research Center, Heidelberg, Germany

Extensive ^{15}N labeling and multiple-stage tandem mass spectrometry were used to investigate the fragmentation pathways of the model peptide FGGFL during low-energy collision-induced-dissociation (CID) in an ion-trap mass spectrometer. Of particular interest was formation of a_4 from b_4 and a_4* (a_4-NH_3) from a_4 ions correspondingly, and apparent rearrangement and scrambling of peptide sequence during CID. It is suggested that the original $FGGF_{oxa}$ b_4 structure undergoes *b*-type scrambling to form $GGFF_{oxa}$. These two isomers fragment further by elimination of CO and $^{14}NH_3$ or $^{15}NH_3$ to form the corresponding $a_4$and a_4* isomers, respectively. For (^{15}N-F)GGFL and FGG(^{15}N-F)L the a_4* ion population appears as two distinct peaks separated by 1 mass unit. These two peaks could be separated and fragmented individually in subsequent CID stages to provide a useful tool for exploration of potential mechanisms along the $a_4 \rightarrow a_4$* pathway reported previously in the literature (Vachet et al. *J. Am. Chem. Soc.* **1997,** *119*, 5481, and Cooper et al. *J. Am. Soc. Mass Spectrom.* **2006,** *17*, 1654). These mechanisms result in formally the same a_4* structures but differ in the position of the expelled nitrogen atom. Detailed analysis of the observed fragmentation patterns for the separated light and heavy a_4* ion fractions of (^{15}N-F)GGFL indicates that the mechanism proposed by Cooper et al. is consistent with the experimental findings, while the mechanism proposed by Vachet et al. cannot account for the labeling data. In addition, a new rearrangement pathway is presented for a_4*-CO ions that effectively transfers the former C-terminal amino acid residue to the N-terminus. (J Am Soc Mass Spectrom 2008, 19, 1788–1798) © 2008 Published by Elsevier Inc. on behalf of American Society for Mass Spectrometry

The primary method used for peptide and protein identification in proteomics is tandem mass spectrometry (MS/MS or MS^2) [1, 2]. In most MS/MS experiments, protonated peptides are excited collisionally to induce dissociation (collision-induced-dissociation, CID) and the fragment ion spectrum is used to elucidate peptide sequences. The CID spectra of peptides in proteomics studies are commonly assigned by bioinformatics tools that implement sequencing algorithms and peptide fragmentation models. Regrettably, the existing sequencing programs are based on rather limited fragmentation models that poorly approximate the rich dissociation chemistry of protonated peptides [3]. These limitations often lead to erroneous assignment of peptides and proteins, and the resulting uncertainty in the evaluation of the raw MS/MS data is one of the major limiting factors in large-scale protein identification studies [4, 5]. The incorporation of more detailed peptide fragmentation mechanisms and spectral characteristics into these sequencing algorithms would undoubtedly place MS/MS based sequencing on a much more robust basis.

In general, fragmentation of protonated peptides under low-energy collision conditions involves proton-driven reactions in which amide bonds are cleaved along the peptide backbone and *b*, *y*, and *a* ions [6, 7] are formed. The energetics and kinetics of the necessary proton mobilization (mobile proton model [8, 9]) and amide bond cleavage pathways [3, 10–14] have received significant research interest. On the other hand, much less attention has been devoted to the structure and reactivity of the primary fragments formed by backbone cleavages. According to the recent pathways in competition (PIC) fragmentation model [3], the thermodynamic properties and the reactivity of these frag-

Address reprint requests to Dr. M. Van Stipdonk, Department of Chemistry, Wichita State University, Wichita, KS, USA, or Dr. B. Paizs, Department of Molecular Biophysics, German Cancer Research Institute, Heidelberg, Germany. E-mail: Mike.VanStipdonk@wichita.edu or B.Paizs@dkfz.de

* Portions of this work were presented at the 55th ASMS Conference on Mass Spectrometry and Allied Topics, June 4–7, Indianapolis, Indiana, USA.

1044-0305/08/$32.00
doi:10.1016/j.jasms.2008.08.010

Published online August 19, 2008
Received July 3, 2008
Revised August 14, 2008
Accepted August 14, 2008

ments play a significant role in the post-cleavage phase of peptide fragmentation and can be used to understand some fragment intensity relationships.

Early studies demonstrated that the C-terminal *y* fragments are truncated peptides and their structure and reactions can be explained based on the chemistry of their parent peptides [3, 14–16]. On the other hand, N-terminal fragments (*b* and *a* ions) show new C-terminal functionalities that are introduced by the initial amide bond cleavage. Ions of the *b* series were originally considered to have the charged acylium group [2]. However, later Harrison and coworkers suggested the oxazolone structure [10, 17], which could explain most of the reactions of *b* ions. The oxazolone structure has found support from IR spectroscopy and modeling [18, 19]. In a recent paper, Harrison and coworkers [20] proposed that oxazolone terminated linear *b* ions can cyclize by nucleophilic attack of the N-terminal amino group on the charged oxazolone ring. This reaction leads to a macro-cyclic *b* isomer [21], the existence of which has recently been demonstrated by Gaskell and coworkers [22] using ion mobility spectroscopy. Cyclic *b* ion structures can in principle open up at any amide bond (*b*-type scrambling) and this reaction can lead to linear isomers with scrambled primary structures. Further fragmentation of such ions results in *non-direct sequence* ions [20] in the MS/MS spectra of protonated peptides.

Other alternative ion structures can be derived if His, Arg, Asp, or Lys occupies the C-terminal position in *b* ions [23–26]. In these cases the side-chain nucleophiles of the preceding amino acids are responsible for cleavage of the amide bond or reisomerization of the primarily formed oxazolone ring. To complicate matters even further, recent statistical studies by Zubarev and coworkers [27] suggest that b_2 ions of doubly protonated tryptic peptides are unusual and might be protonated diketopiperazines. The structure of *b* fragments is still heavily debated (see contributions from Harrison, Zubarev, and Gaskell in this focus issue) and further studies are needed to answer a number of open questions in this respect.

Comparatively little is known about the structure and reactivity of *a* and *a** ions. The former are assumed to have imine groups at their C-terminus and can be formed from *b* ions by loss of CO [10] or directly from protonated peptides [28]. Under low-energy collision conditions, the first reaction is preferred. Harrison and coworkers have studied formation [10] of *a* ions from *b* fragments with assumed oxazolone structures (study of the formation of *a* fragments from alternative *b* structures still awaits). Their kinetic energy release measurements indicate CO loss occurs through a high barrier and the product energy level is below that of the transition structure involved. A mechanism that fits these experimental characteristics was proposed by Paizs and coworkers [29] based on quantum chemical calculations.

Vachet et al. discovered [30] that the $a \rightarrow a^*$ ($a\text{-}NH_3$) pathway involves a rearrangement of the former C-terminal residue to the N-terminus. For example, CID of protonated leu-enkephalin (YGGFL) under some circumstances results in the $a_4\text{-}NH_3\text{-}G$ fragment at *m/z* 323 that is formed from the a_4 ion by losing ammonia and one of the formerly internal Gly residues. In recent work [19], Polfer et al. studied the structure of the a_4 of YGGFL using IR spectroscopy and modeling. This study indicated that the linear a_4 isomer is protonated at the N-terminal amino group and the C-terminal imine is in the *trans* isomerization state. Furthermore, a cyclic isomer formed by nucleophilic attack of the N-terminal amino group on the charged imine carbon exists. Quantum chemical calculations indicated that the cyclic form is energetically more favored than the linear structures. Ion mobility experiments [22, 31] confirmed that *a* ions have multiple structures. A recent CID and theoretical study [32] from our laboratories indicated that the CID spectra of a_5 fragments of YAGFL-NH_2 can reasonably be understood by assuming an interplay of *b*-type scrambling [20] of the corresponding *b* parent population and $a \rightarrow a^*$ type rearrangements [30].

The present study reports a combined CID, labeling, and computational study of the structure and reactions of *a* and *a** ions. Multiple-stage CID of unlabeled FGGFL, and versions of the peptide bearing ^{15}N and α-d_2 isotope labels, were used to examine the fragmentation and in particular the apparent rearrangement of sequence of this model peptide. This specific sequence was chosen as a good compromise between reproduction of past CID results for YGGFL and reasonable cost of synthesis of a series of isotope labeled peptides.

Experimental and Computational Details

Experimental work was performed at the Department of Chemistry, Wichita State University, Wichita, Kansas. The molecular dynamics simulations and the quantum chemical calculations were carried out at the German Cancer Research Center in Heidelberg. Both the experimental and theoretical strategies are briefly described below.

Mass Spectrometry

All labeled and unlabeled versions of FGGFL were generated by conventional solid-phase synthesis methods [33] using 9-fluorenylmethoxycarbonyl (Fmoc)-glycine loaded Wang resin (Sigma Chemical, St. Louis, MO) and a custom-built, multiple reaction vessel peptide synthesis apparatus. Fmoc-protected glycine (G), phenylalanine (F), glycine-^{15}N ($H_2{}^{15}NCH_2COOH$, **G-^{15}N**), phenylalanine-^{15}N ($H_2{}^{15}NCH(CH_2C_6H_5)COOH$, **F-^{15}N**) and leucine (L)-loaded Wang resin were purchased from Sigma Chemical and used as received. Peptides, once cleaved from the resin, were used without subsequent purification in the CID studies. Peptide sequence, and in particular the position of isotope labels, was confirmed using multiple-

stage CID of Na^+ and Ag^+ cationized versions (which is an effective approach for sequencing from the C-terminus in the gas-phase [34]). Solutions of each peptide were prepared by dissolving the appropriate amount of solid material in a 1:1 (vol:vol) mixture of HPLC grade MeOH (Aldrich Chemical, St. Louis, MO) and deionized H_2O to produce final concentrations of 10^{-5}-10^{-4} M.

ESI mass spectra were collected using a Finnigan LCQ-Deca ion-trap mass spectrometer (Finnigan, CA, USA). Peptide solutions were infused into the ESI-MS instrument using the incorporated syringe pump and a flow rate of 5 μL/min. The atmospheric pressure ionization stack settings for the LCQ (lens voltages, quadrupole and octopole voltage offsets, etc.) were optimized for maximum $(M + H)^+$ transmission to the ion trap mass analyzer by using the auto-tune routine within the LCQ Tune program. Following the instrument tune, the spray needle voltage was maintained at +5 kV, the N_2 sheath gas flow at 25 units (arbitrary for the Finnigan systems, corresponding to ~0.375 L/min) and the capillary (desolvation) temperature at 200 °C. Helium was used as the bath/buffer gas to improve trapping efficiency and as the collision gas for CID experiments.

The CID studies (MS/MS and MS^n) were performed as follows. The $(M + H)^+$ ions were isolated for the initial CID stage (MS/MS) using an isolation width of 0.9 to 1.2 mass to charge (*m/z*) units. Product ions selected for subsequent CID (MS^n experiments) were isolated using widths of 1.0 to 1.3 *m/z* units. The exact width was chosen empirically and reflected the best compromise between high precursor ion abundance and the isolation of a single isotopic peak. The (mass) normalized collision energy, which defines the amplitude of the r.f. energy applied to the end cap electrodes in the CID experiment, was set between 20% and 25%, which corresponds roughly to 0.55–0.68 V with the instrument calibration used in this study). The activation Q (as labeled by ThermoFinnigan, used to adjust the q_z value for the precursor ion) was set at 0.30. Subsequent CID stages were performed using similar activation parameter settings. The activation time employed at each CID stage was 30 ms.

Computational Details

The potential energy surface (PES) of the FG_GFim a*-CO fragment (an ion that features the CHR═N-CHR'—CO— moiety (denoted by XY_) at the N-terminus) derived from the $GGFF_{oxa}$ b_4 ion was investigated using the strategy developed recently to deal with protonated peptides [3, 35]. These calculations began with molecular dynamics simulations using the Insight II program (Biosym Technologies, San Diego, CA) in conjunction with the AMBER force field [36], modified in-house to enable the study of oxygen and nitrogen protonated amide bonds and amide bond cleavage transition structures (TS). During the dynamics calculations we used simulated annealing techniques to produce candidate structures for further refinement, applying full geometry optimization using the AMBER force field. These optimized structures were analyzed by a conformer family search program developed in-house. This program groups optimized structures into families for which the most important characteristic torsion angles of the molecule are similar. The most stable species in the families were then fully optimized at the PM3, HF/3-21G, B3LYP/6-31G(d), and finally at the B3LYP/6-31+G(d,p) levels, and the conformer families were regenerated at each level. The Gaussian set of programs [37] was used for all ab initio and DFT calculations.

For the energetically most preferred structures, we performed frequency calculations at the B3LYP/6-31G(d) level of theory. The relative energies were calculated by correcting the B3LYP/6-31+G(d,p) total energies for zero-point vibrational energy (ZPE) contributions determined from the unscaled B3LYP/6-31G(d) frequencies.

Results and Discussion

CID and Fragmentation Pathways of FGGFL

Figure 1 shows the multiple-stage CID spectra generated from protonated FGGFL. CID (MS/MS stage) of $(M + H)^+$ at *m/z* 540 (Figure 1a) produced b_4 at *m/z* 409, and the $(M - H_2O + H)^+$, a_4 and y_3 ions at *m/z* 552, 381, and 336, respectively. The dominant product ion generated by subsequent CID of b_4 (MS^3 stage, Figure 1b) was the a_4 ion at *m/z* 381. Also observed were peaks at *m/z* 364 and 262. The peak at *m/z* 364 is 17 mass units (u) lower than the a_4 ion, and corresponds to formation of the a_4* (a_4-NH_3) ion [38]. The peak at *m/z* 262 represents the elimination of 147 u, corresponding to the residue mass of F, to form b_3. Isolation and dissociation of a_4 at *m/z* 381 (MS^4 stage, Figure 1c) led primarily to the a_4* peak at *m/z* 364, the b_3 ion at *m/z* 262, with additional peaks at *m/z* 307, 234, and 217. The peak at *m/z* 307 corresponds to elimination of 57, or G from a_4*. The peaks at *m/z* 234 and 217 are formed by elimination of 147 u from $a_4$and a_4*, respectively. Fragmentation of a_4* at *m/z* 364 (MS^5 stage, Figure 1d) led to formation of the peaks at *m/z* 336 (a_4*-CO), 307 (a_4*-G), 222 and 217 (a_4*-F).

In general, the product ions generated in the multiple-stage CID of FGGFL are consistent with those reported by Vachet et al. [30], and subsequently by Barr and Van Stipdonk [34] for YGGFL. Of particular interest were the prominent a_4 and a_4* peaks, a_4* created by dissociation of a_4 and also the subsequent elimination of 57 and 147 u from a_4*. The latter clearly suggests that the a_4* ion population consists of two isomers, one losing F and the other eliminating G upon CID. Clearly, this observation is in line with our recent proposal [32] on the interaction of *b*-type scrambling and the $a \rightarrow a^*$ rearrangement pathway. The original $FGGF_{oxa}$ b_4 ion can undergo cyclization and subsequent ring opening [20] to form other linear struc-

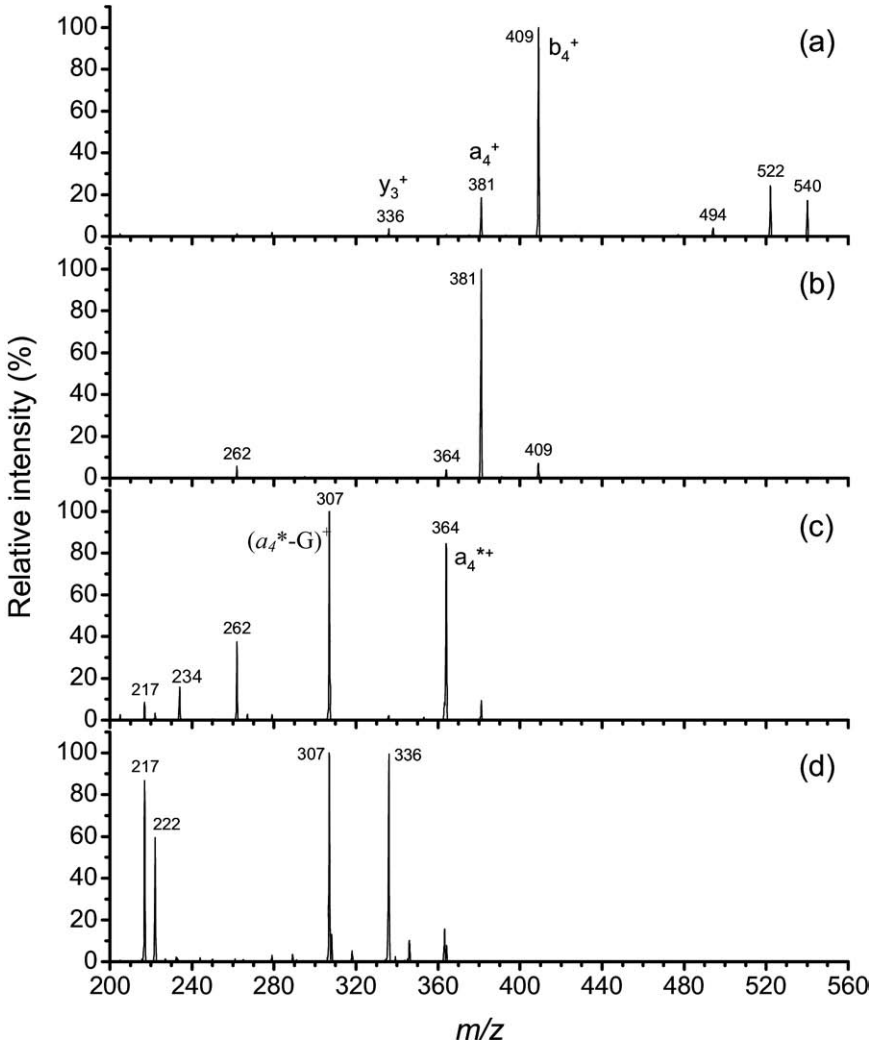

Figure 1. Multiple-stage CID spectra derived from protonated FGGFL: (**a**) CID (MS/MS) of $(M + H)^+$, (**b**) CID (MS^3) of b_4, (**c**) CID (MS^4) of a_4, (**d**) CID (MS^5) of a_4*.

tures like $GGFF_{oxa}$, $GFFG_{oxa}$, and $FFGG_{oxa}$. CID of the b_4 ion population (Figure 1b) leads to the b_4-*F* peak, the b_4-*G* fragment at *m/z* 352 is not observed. This suggests that the b_4 isomers $GFFG_{oxa}$ and $FFGG_{oxa}$ are unlikely to be formed in the scrambling process because their subsequent fragmentation would result in formation of the b_4-*G* fragment. This speculation is supported by computational data on the $YGGF_{oxa}$, $GGFY_{oxa}$, $GFYG_{oxa}$, and $FYGG_{oxa}$ linear b_4 isomers derived from YGGFL (B. Paizs, unpublished results). These indicate that $GGFY_{oxa}$ and $YGGF_{oxa}$ are energetically more favored than $GFYG_{oxa}$ and $FYGG_{oxa}$, so ring-opening pathways that place G to the C-terminus of the linear isomers appear to be thermodynamically controlled. Consequently, in the following we assume that the b_4 population consists of the $FGGF_{oxa}$ and $GGFF_{oxa}$ linear isomers.

Two major mechanisms have been proposed for the $a \rightarrow a^*$ rearrangement pathway. In their original study, Vachet and Glish suggested [30] that the a_4* ion was formed via a S_N2 type reaction involving attack by the C-terminal imine group on the N-terminal α-carbon forming a cyclic a_4* ion as the N-terminal NH_3 is lost (worked out for the $FGGF_{oxa}$ and $GGFF_{oxa}$ isomers in Scheme **1**). Subsequent opening of the macro-ring leads to a rearranged sequence and further fragmentation can result in loss of the formerly internal residue. The linear a_n* ions feature the CHR═N-CHR′—CO— moiety (denoted by XY_) at their N- and an oxazolone group at their C-terminus, respectively. The CHR═N-CHR′—CO— moiety is likely to be more stable than the C-terminal oxazolone group, therefore dissociation of a_n* ions is likely to be dominated by gradual degradation at their C-terminus. Such a fragmentation pathway explains loss of the internal G residues from the *a* ions like $FGGF_{im}$ and $YGGF_{im}$.

An alternative mechanism proposed recently by us [39, 40] is shown on Scheme **2**. (A similar mechanism was proposed by Uggerud and coworkers for elimination of ammonia from glycinamide [41].) This mechanism involves cleavage of the C-terminal–CO-NH^+ bond by nucleophilic attack of the N-terminal adjacent amide oxygen on the carbonyl carbon. This reaction

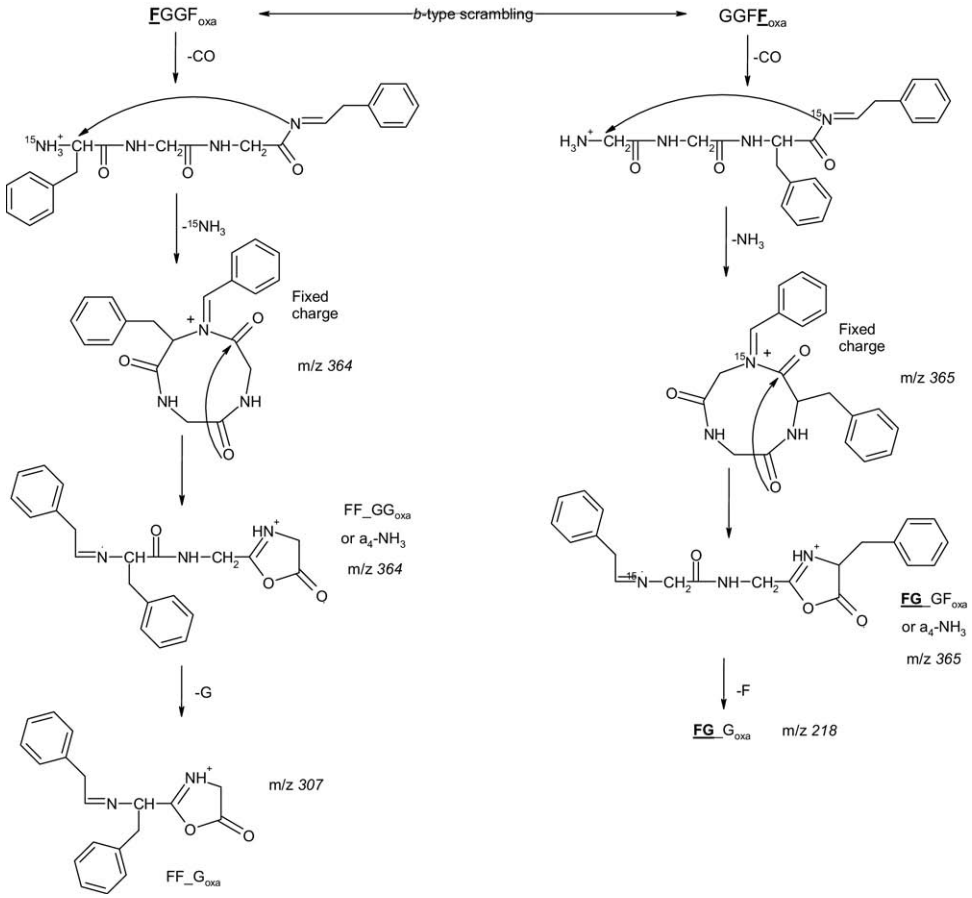

Scheme 1. A reaction pattern for the b_4 ion of FGGFL that combines *b*-type scrambling of the $FGGF_{oxa}$ structure to form $GGFF_{oxa}$ and the Vachet-Glish mechanism of the $a \rightarrow a^*$ pathway. This reaction pattern is presented for the b_4 fragments derived from (^{15}N-F)GGFL. The ^{15}N isotope is explicitly labeled in the chemical structures while the isotope-labeled phenylalanine residues are noted as ***F*** (bold and underlined) in the shorthand notations like $\mathbf{\underline{F}}GGF_{oxa}$; *m/z* values of the various ions are noted in italics.

leads to the next lower *b* ion that is terminated by an oxazolone ring at its C-terminus (FGG_{oxa} in Scheme **2**) and the imine of the former C-terminal residue. Under low-energy CID conditions these two fragments form a proton-bound dimer (PBD), which can undergo proton transfer to the imine monomer and subsequent re-association via nucleophilic attack of the N-terminal amine on the protonated imine creating a new N-terminus. This reaction effectively transfers the formerly C-terminal residue to the N-terminus, thus creating new functionalities at both termini. Loss of ammonia occurs after proton transfer to the new N-terminal amino group leaving behind the CHR═N-CHR′—CO— moiety.

The Vachet-Glish (VG) and the PBD mechanisms of the $a \rightarrow a^*$ rearrangement pathway lead to final products that are formally the same (Schemes **1** and **2**), via expulsion of ammonia. However, the VG and the PBD mechanisms involve elimination of different nitrogen atoms, the N-terminal or the C-terminal nitrogens, respectively. To decipher which mechanism was responsible for the $a \rightarrow a^*$ rearrangement pathway, we synthesized isotopically-labeled variants of FGGFL, systematically varying the position of ^{15}N along the backbone. With these peptides, the pattern with respect to retention or elimination of the ^{15}N as part of the departing NH_3 molecule could be observed to help elucidate which mechanism is responsible for the $a \rightarrow a^*$ rearrangement pathway.

The CID spectra (MS^4 stage) generated by isolation and collisional activation of a_4 of unlabeled FGGFL, (^{15}N-F)GGFL, F(^{15}N-G)GFL, FG(^{15}N-G)FL, and FGG(^{15}N-F)L, are shown in Figure 2. Note that only portions of those spectra, focused on the *m/z* range that includes the a_4^* ion, collected using the higher resolution, Zoomscan function of the LCQDeca platform, are displayed. For the unlabeled peptide, and F(^{15}N-G)GFL and FG(^{15}N-G)FL, formation of a_4^* from a_4 involved primarily the elimination of $^{14}NH_3$. For example, the a_4^* ion appears at *m/z* 364 when generated from a_4 (*m/z* 381) derived from (unlabeled) FGGFL. Likewise, the a_4^* species appears at *m/z* 365 when generated from a_4 (*m/z* 382) derived from either F(^{15}N-G)GFL or FG(^{15}N-G)FL. Conversely, the a_4^* species appears as two peaks separated

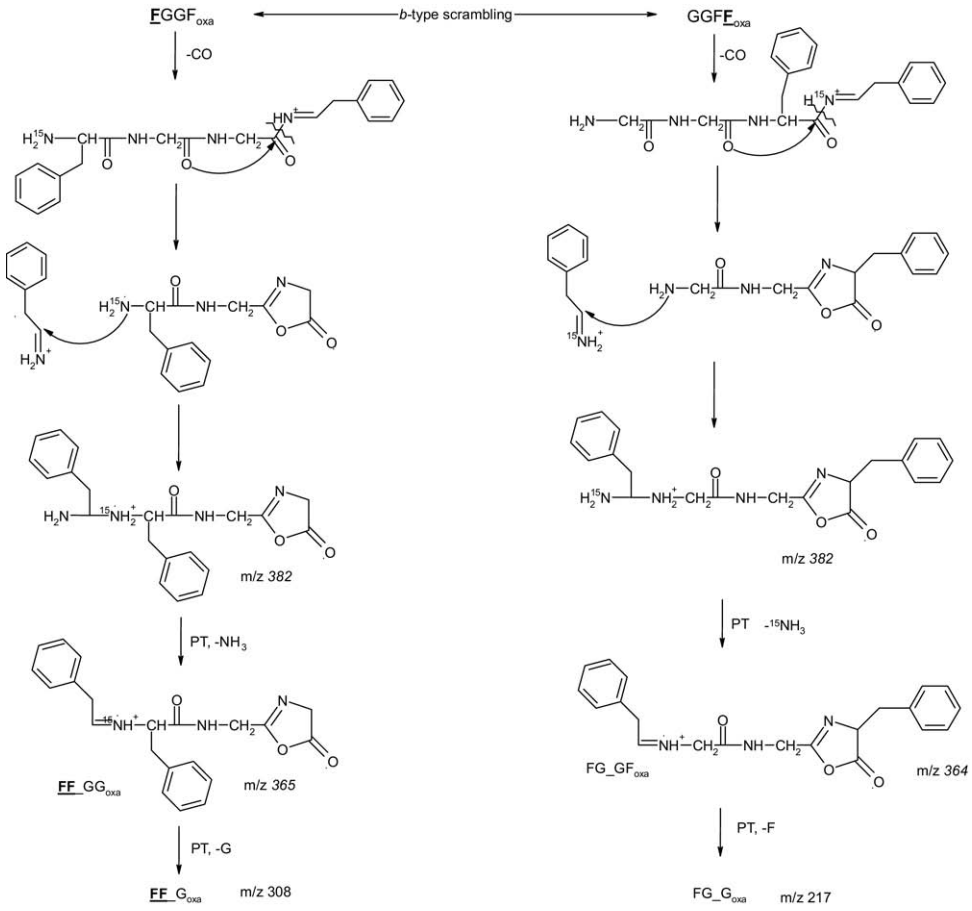

Scheme 2. A reaction pattern for the b_4 ion of FGGFL that combines *b*-type scrambling of the FGGF$_{oxa}$ structure to form GGFF$_{oxa}$ and the PBD mechanism of the $a \rightarrow a^*$ pathway. This reaction pattern is presented for the b_4 fragments derived from (^{15}N-F)GGFL. The ^{15}N isotope is explicitly labeled in the chemical structures while the isotope-labeled phenylalanine residue is noted as ***F*** (bold and underlined) in the shorthand notations like ***F***GGF$_{oxa}$; *m/z* values of the various ions are noted in italics.

by 1 u when generated from the a_4 ion derived from either (^{15}N-F)GGFL or FGG(^{15}N-F)L.

The observation of split a_4* peaks can be explained in three ways. The first argument would be that formation of a_4* involves two distinct pathways (the VG and the PBD mechanisms), one that involves elimination of the N-terminal amino group and one that eliminates the N atom of the initially C-terminal amide group. Another feasible explanation is that two isomers (FGGF$_{oxa}$ and GGFF$_{oxa}$) are formed in *b*-type scrambling of the parent b_4 population and the position of the labeled residue changes due to the scrambling process. Finally, these two effects can in principle interact leading to four different cases: FGGF$_{oxa}$ and GGFF$_{oxa}$ can both be present in the mass spectrometer and they can fragment further on the VG and/or the PBD pathway.

The apparent generation of two distinct a_4* fractions from (^{15}N-F)GGFL or FGG(^{15}N-F)L provided an opportunity to examine each case individually. Figure 3 shows the CID spectra (MS5 stage) generated by isolation of a_4* from FGGFL (Figure 3a), FGG(^{15}N-F)L (Figure 3b and c), and (^{15}N-F)GGFL (Figure 3d and e). The two distinct fragmentation patterns observed in Figure 3 clearly suggest that different forms of a_4* (isolated at *m/z* 364 and 365) exist, and these ions exhibit very different chemical behavior. In the following we will concentrate on the last two panels of Figure 3 and analyze the chemistry of the a_4* ions derived from (^{15}N-F)GGFL.

Scheme **1** displays the reaction pattern derived by combining the *b*-type scrambling and VG $a \rightarrow a^*$ pathways. ***F***GGF$_{oxa}$ (the ***X*** shorthand notation is used to note an ^{15}N labeled residue here) loses CO and then ^{15}NH$_3$ on the VG pathway to form the a_4* ion with the FF_GG$_{oxa}$ composition at *m/z* 364. The *m/z* 364 fraction of the a_4* ion population (Figure 3e) fragments by losing CO to form a_4*-CO and by eliminating F to form *m/z* 217 (formation of the ion at *m/z* 222 will be discussed separately in section 3.2). The a_4* ion structure of FF_GG$_{oxa}$ as proposed by the VG mechanism would however eliminate G from its C-terminus to form FF_G$_{oxa}$ at *m/z* 307. No such ion is observed in Figure 3e suggesting that the a_4* ion population derived from ***F***GGF$_{oxa}$ is not formed on the VG $a \rightarrow a^*$ pathway.

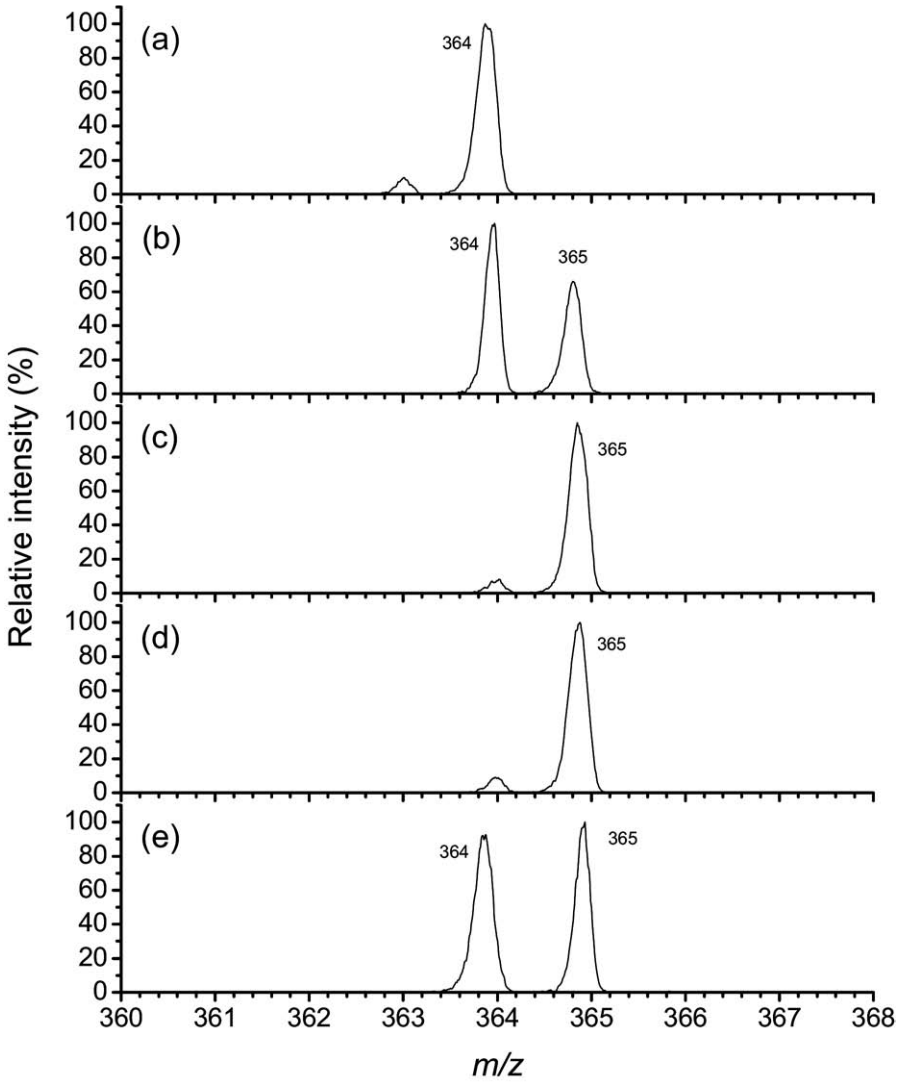

Figure 2. CID (MS^4 of a_4 derived from unlabeled FGGFL, and the group of 15N labeled versions of the peptide: (**a**) FGGFL, (**b**) FGG(^{15}N-F)L, (**c**) FG(^{15}N-G)FL, (**d**) F(^{15}N-G)GFL, and (**e**) (^{15}N-F)GGFL.

The GGF$\boldsymbol{F}_{oxa}$ b_4 isomer is formed from $\boldsymbol{F}$GGF$_{oxa}$ by cyclization and subsequent reopening. Note that the labeled phenylalanine residue is relocated to the C-terminus by this chemistry. GGF$\boldsymbol{F}_{oxa}$ loses CO and then $^{14}NH_3$ on the VG pathway and forms the a_4* ion with the $\boldsymbol{FG}$_GF$_{oxa}$ composition at *m/z* 365. According to Figure 3d, the *m/z* 365 fraction of the a_4* ion population fragments to form ions at *m/z* 337 and 308. On the other hand, $\boldsymbol{FG}$_GF$_{oxa}$ is expected to fragment by eliminating the C-terminal F to form $\boldsymbol{FG}$_G$_{oxa}$ at *m/z* 218. No such ion is observed in Figure 3d, suggesting that the a_4* ion population derived from GGF$\boldsymbol{F}_{oxa}$ is not formed on the VG $a \rightarrow a$* pathway.

Scheme **2** displays the reaction pattern derived by combining the *b*-type scrambling and PBD $a \rightarrow a$* pathways. $\boldsymbol{F}$GGF$_{oxa}$ loses CO and then $^{14}NH_3$ on the PBD pathway to form the a_4* ion with the $\boldsymbol{FF}$_GG$_{oxa}$ composition at *m/z* 365. The *m/z* 365 fraction of the a_4* ion population fragments (Figure 3d) by losing CO to form a_4*-CO, *m/z* 337, and by eliminating G to form *m/z* 308. The a_4* ion structure of $\boldsymbol{FF}$_GG$_{oxa}$ as proposed by the PBD mechanism for *m/z* 365 most likely eliminates G from its C-terminus to form $\boldsymbol{FF}$_G$_{oxa}$ at *m/z* 308. This ion is observed in Figure 3d, clearly suggesting that the a_4* ion population derived from $\boldsymbol{F}$GGF$_{oxa}$ can be formed on the PBD $a \rightarrow a$* pathway. Elimination of the specific G residue shown in Scheme **2** to produce the *m/z* 308 product was confirmed using peptides with both ^{15}N and (glycine) α-d_2 isotope labels (spectra not shown). We found that the loss of 57 u shifted to loss of 59 when (^{15}N-F)G(α-d_2-G)FL was used as the precursor peptide. The loss remained at 57 u when (^{15}N-F)(α-d_2-G)GFL was used as the precursor peptide instead. Therefore, use of the doubly-labeled peptides allows us to conclude that the residue eliminated to create the species at 307 or 308 in Figure 3d and e, respectively, is the C-terminal most G.

The GGF$\boldsymbol{F}_{oxa}$ b_4 isomer is formed from $\boldsymbol{F}$GGF$_{oxa}$ by *b*-type scrambling and the labeled phenylalanine resi-

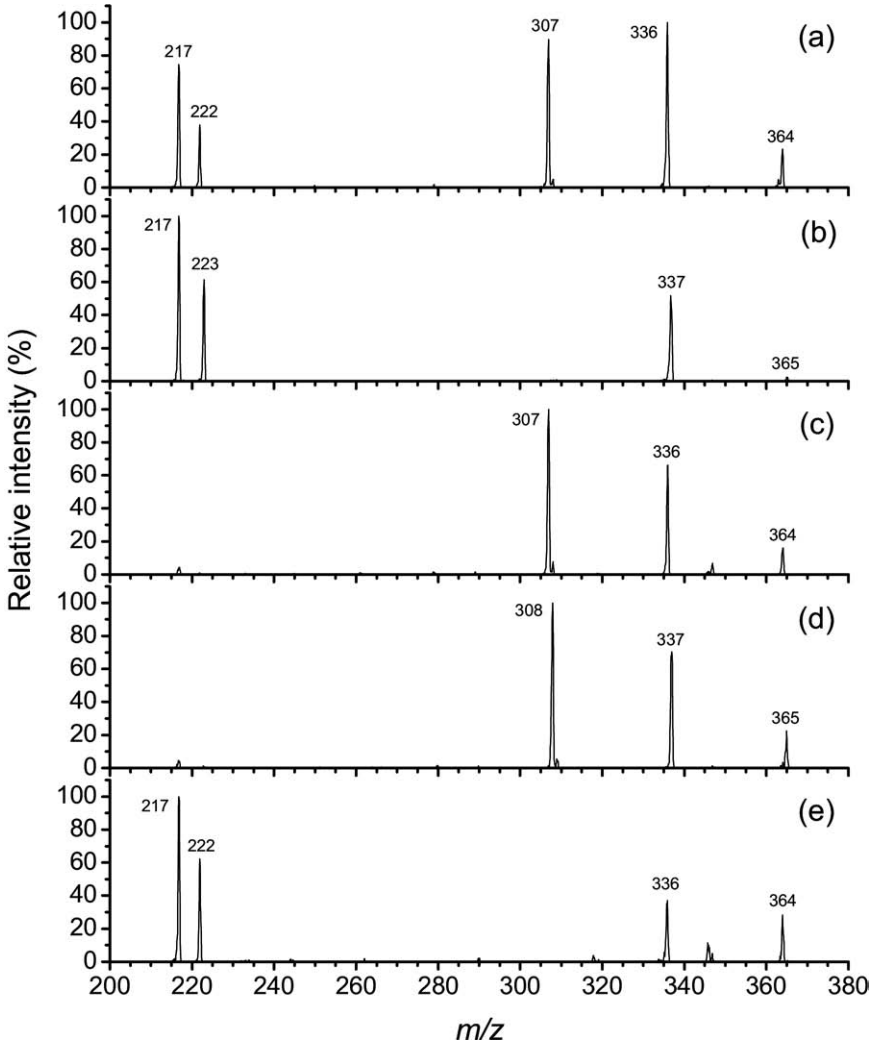

Figure 3. CID spectra (MS^5 stage) generated by isolation of a_4* from (unlabeled) FGGFL (**a**), (15N-F)GGFL (**b**) and (**c**) and FGG(15N-F)L (**d**) and (**e**).

due gets relocated to the C-terminus in this rearrangement. The GGF***F***$_{oxa}$ b_4 isomer loses CO and then $^{15}NH_3$ on the PBD pathway to form the a_4* ion with the FG_GF$_{oxa}$ composition at *m/z* 364. According to Figure 3e, the *m/z* 364 fraction of the a_4* ion population fragments to form ions at *m/z* 336 and 217. The FG_GF$_{oxa}$ ion structure proposed by the PBD mechanism for *m/z* 364 most likely eliminate F from its C-terminus to form FG_G$_{oxa}$ at *m/z* 217. This ion is observed in Figure 3e clearly suggesting that the a_4* ion population derived from GGF***F***$_{oxa}$ can be formed on the PBD $a \rightarrow a^*$ pathway.

The preceding analysis of the fragmentation patterns of the isolated *m/z* 364 and 365 a_4* populations of (^{15}N-F)GGFL strongly suggests that the $a \rightarrow a^*$ reaction involves the PBD mechanism. The plausibility of the PBD mechanism is also supported by similar analysis of the corresponding FGG(^{15}N-F)L data (Schemes **1** and **2** in the Supplementary Data, which can be found in the electronic version of this article), which reach the same conclusion, that the a_4* ions are formed according to the PBD chemistry. It should be noted however that while supporting the PBD mechanism, the FGG(^{15}N-F)L data are unable to definitively exclude the VG mechanism.

A reviewer has suggested that a direct pathway involving concerted loss of G and NH_3 form the a_4 ion (loss of H_2N-CH_2-CO-NH_2) could also be the source of the a_4*-*G* peak (*m/z* 307) in Figure 1. The main argument behind this proposal is that the CID spectra displayed in Figure 1c and d show significantly different intensities for the peak that correspond to loss of CO from a_4. The very low intensity of the peak at *m/z* 336 in Figure 1c could appear to suggest that there exists a separate pathway to elimination of G and NH_3 (nominally C_2H_6NO) directly from a_4, without passing through the a_4*-*CO* species. Identification of such a direct pathway would best be done using a double-resonance experiment with a short timescale, which we are currently not equipped to perform.

However, this phenomenon can be explained by considering the energetics of the $a_n \rightarrow a_n^*$ and $a_n^* \rightarrow$

a_n*-*X* (X is the eliminated amino acid residue) fragmentation channels that is sketched for the present case in Figure S1 of the Supporting Data. Our calculations on a_5 of YAGFL [32] suggest that the highest TS on the $a \rightarrow a^*$ multi-step pathway is around 20 kcal/mol and the relative energy of a_4* is around 10 kcal/mol. The latter has an oxazolone C-terminus, the fragmentation energetics of which has recently been studied [42]. These studies indicate that the CO-loss and subsequent imine-loss TSs have very similar threshold energies and the final a_4*-*G* level is just slightly above those of these TSs (Figure S1 of the Supporting Data). Consequently, the energetics suggest that the less energized part of the a_4 population fragments to form a_4* while the high-energy tail is not likely to be observed as a_4*-*CO*, these species will fragment further to a_4*-*G*. On the other hand, the low-energy species of the a_4* population are likely to be observed as a_4*-*CO*, and only the high-energy tail will fragment further to form a_4*-*G*. These considerations clearly explain why a_4*-*CO* is not observed in Figure 1c while this is the main peak in Figure 1d without introducing a new direct $a \rightarrow a^*$-X mechanism.

*Formation of the m/z 222 Fragment of a_4**

Figure 3a shows formation of an ion at *m/z* 222 that appears in panels 3b (shifted by 1 u to *m/z* 223) and 3e too. Our analysis above suggested that a_4* ions are formed on the PBD $a \rightarrow a^*$ pathway and the *m/z* 364 fraction of the a_4* population of (^{15}N-F)GGFL is FG_GF$_{oxa}$ formed

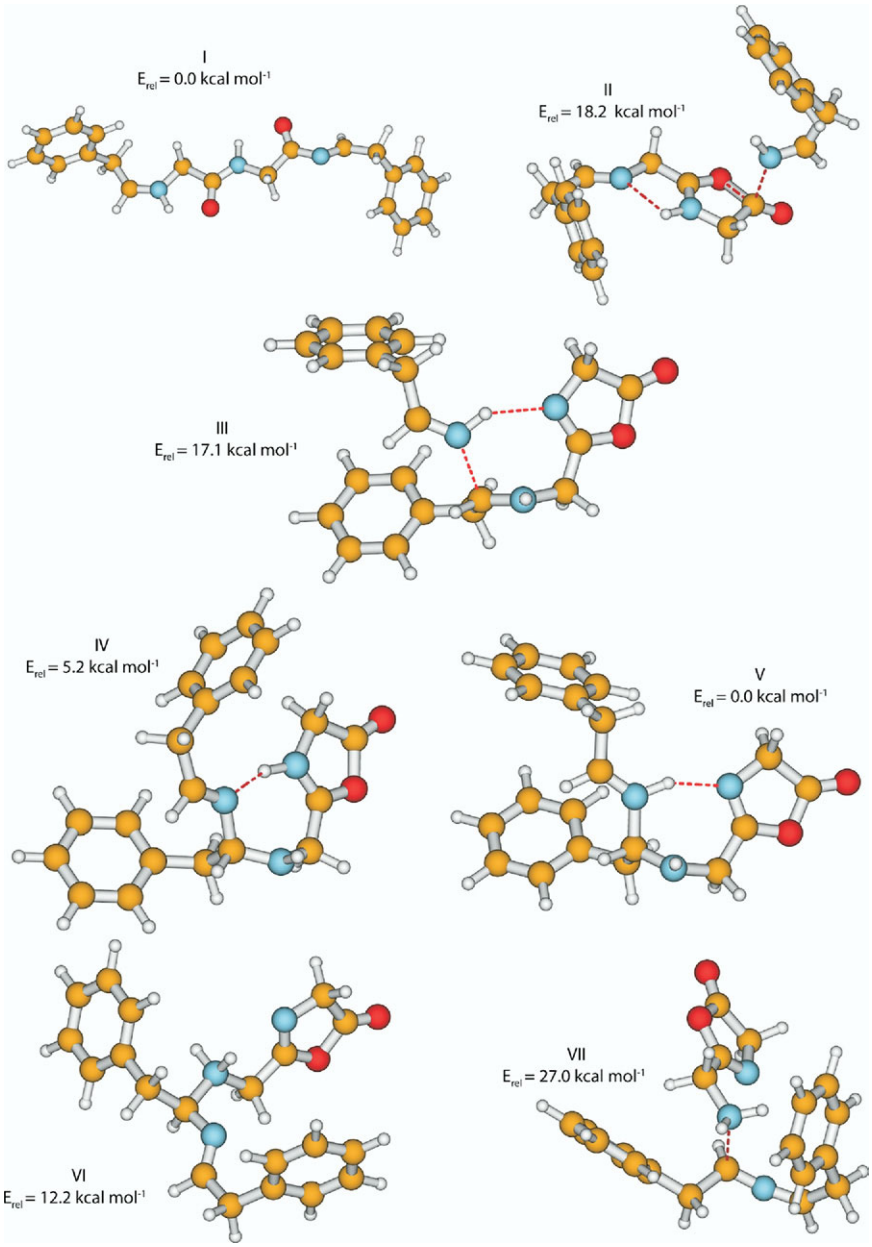

Figure 4. Various structures on the FG_GF$_{im}$ PES (relative energies are included for clarity).

from the GGF$\boldsymbol{F}_{oxa}$ b_4 isomer. According to Figure 3 FG_GF_{oxa} loses CO (to form FG_GF_{im} at *m/z* 336) and F to form FG_G_{oxa} at *m/z* 217 and forms the ion at *m/z* 222. This ion can be assigned as C_6H_5—CH_2—CH═N^+═CH—CH_2—C_6H_5, a structure that contains a fixed charge at the central nitrogen. This ion is formed from FG_GF_{im} where the two phenylalanines occupy the N- and C-terminal positions (Structure I in Figure 4). This suggests that formation of the *m/z* 222 fragment takes place on a complex rearrangement pathway (Scheme **3**).

Nucleophilic attack of the FG_ glycine carbonyl oxygen of FG_GF_{im} on the C-terminal carbonyl carbon initiates formation of a new oxazolone ring and cleavage of the C-terminal amide bond. The corresponding transition structure (TS) is shown in Figure 4 as Structure II. The relative energy (E_{Rel}) of this TS compared with the energetically most favored FG_GF_{im} structure is 18.2 kcal mol^{-1}. This reaction produces various proton bound dimers of FG_G_{oxa} and the phenylalanine imine. These fragments can re-associate in the PDB via a TS (17.1 kcal mol^{-1} relative energy, Figure 4, Structure III) to form F_F_GG_{ox} (isomer of FG_GF_{im}, Scheme **3**, the X_Y_ notation is used for RCH═N-R'CH—). F_F_G-G_{ox} can undergo numerous proton transfer reactions (Structures IV, V, VI, at 5.2, 0.0, and 12.2 kcal mol^{-1} E_{Rel}, Figure 4). The last of these (Structure VI) fragments to form the ion at *m/z* at 222 through a TS at 27.0 kcal mol^{-1} (Structure VII, Figure 4). To the best of our knowledge, this is the first report of such an ion. The mechanism of Scheme **3** can easily be adapted to explain formation of the *m/z* 223 ion in Figure 3b from the a_4* ion of FGG(^{15}N-F)L where the ^{15}N is incorporated in the F_F ion (S**I** Scheme S**4**). The chemistry shown in Scheme **3** effectively transfers the former C-terminal amino acid residue to the N-terminus.

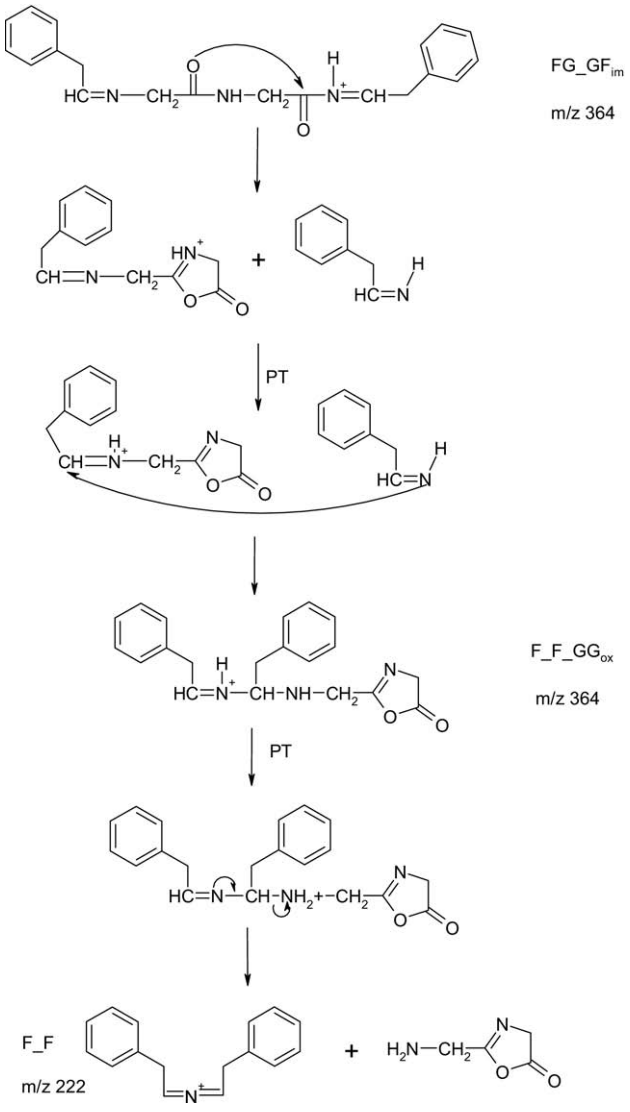

Scheme 3. A rearrangement pathway for the a_4 *-CO fragments of (^{15}N-F)GGFL shown from the FG_GF_{im} structure.

Conclusions

We have described here an investigation of the fragmentation of the model peptide FGGFL that was conducted using extensive ^{15}N and ^{2}H labeling and multiple-stage tandem mass spectrometry under low-energy CID conditions in a quadrupole ion-trap mass spectrometer. Of particular interest in this study was formation and further dissociation of the a_4 and a_4* (a_4-NH_3) fragments, and apparent rearrangement and scrambling of peptide sequence during multiple-stage CID. With respect to the retention or elimination of the ^{15}N labels, the patterns observed indicate that formation of a_4* can occur through different structures and distinct pathways. For (^{15}N-F)GGFL and FGG(^{15}N-F)L, the a_4* ion population appears as two distinct peaks separated by 1 mass unit. These peaks could be separated and fragmented individually providing useful information about the chemical structure of these two fractions of the *a** population. Careful analysis of the observed fragmentation patterns indicate that *b*-type scrambling of the parent b_4 population leads to a mixture of FGGF_{oxa} and GGFF_{oxa}, and the *a** ions are formed on the PBD $a \rightarrow a^*$ pathway. It was also shown that *a*-CO* ions can rearrange as well, on a pathway that effectively transfers the former C-terminal amino acid residue to the N-terminus.

Acknowledgments

The authors acknowledge support for this work by grants to M.V.S. from the National Science Foundation (CAREER-0239800) and the Kansas Technology Enterprise Corporation/Kansas NSF EPSCoR program and a Faculty Scholar Award from the Kansas Biomedical Research Infrastructure Network. B.P. is indebted to the Deutsche Forschungsgemeinschaft (SU 244/3-1) for financial support. B.B. thanks the DKFZ for a post-doctoral fellowship.

References

1. Hunt D. F.; Yates, J. R. III; Shabanonowitz J.; Winston S.; Hauer C. R. Protein Sequencing by Tandem Mass Spectrometry. *Proc. Natl. Acad. Sci. U.S.A.* **1986,** *83,* 6233–6237.

2. Biemann, K. Contributions of Mass Spectrometry to Peptide and Protein Structure. *Biomed. Environ. Mass Spectrom.* **1988,** *16,* 99–111.
3. Paizs, B.; Suhai, S. Fragmentation Pathways of Protonated Peptides. *Mass Spectrom. Rev.* **2004,** *24,* 508–548.
4. Steen, H.; Mann, M. The abc's and the xyz's of Peptide Sequencing. *Nat. Rev. Mol. Cell. Biol.* **2004,** *5,* 699–711.
5. Nesvizhskii, A. E.; Vitek, O.; Aebersold, R. Analysis and Validation of Proteomic Data Generated by Tandem Mass Spectrometry. *Nat. Methods* **2007,** *4,* 787–797.
6. Roepstorff, P.; Fohlmann, J. Proposal for a Common Nomenclature for Sequence Ions in Mass Spectra of Peptides. *J. Biomed. Mass Spectrom.* **1984**, *11601.*
7. Biemann, K. Contributions of Mass Spectrometry to Peptide and Protein Structure. *Biomed. Environ. Mass Spectrom.* **1988,** *16,* 99.
8. Dongré, A. R.; Jones, J. L.; Somogyi, Á.; Wysocki, V. H. Influence of Peptide Composition, Gas-Phase Basicity and Chemical Modification on Fragmentation Efficiency: Evidence for the Mobile Proton Model. *J. Am. Chem. Soc.* **1996,** *118,* 8365–8374.
9. Wysocki, V. H.; Tsaprailis, G.; Smith, L. L.; Breci, L. A. Mobile and Localized Protons: A Framework for Understanding Peptide Dissociation. *J. Mass Spectrom.* **2000,** *35,* 1399–1406.
10. Yalcin, T.; Csizmadia, I. G.; Peterson, M. B.; Harrison, A. Why are b-Ions Stable Species in Peptide Spectra? *J. Am. Soc. Mass Spectrom.* **1996,** *7,* 233–242.
11. Paizs B.; Lendvay G.; Vékey K.; Suhai, S. Formation of b_2^+ Ions from Protonated Peptides: An ab Initio Study. *Rapid Commun. Mass Spectrom.* **1999,** *13,* 525–533.
12. Paizs, B.; Suhai, S. Towards Understanding the Tandem Mass Spectra of Protonated Oligopeptides. 1: Mechanism of Amide Bond Cleavage. *J. Am. Soc. Mass Spectrom.* **2004,** *15,* 103–113.
13. Paizs, B.; Suhai, S. Combined Quantum Chemical and RRKM Modeling of the Main Fragmentation Pathways of Protonated GGG. II. Formation of b_2, y_1, and y_2 ions. *Rapid Commun. Mass Spectrom.* **2002,** *16,* 375–389.
14. Polce, M. J.; Ren, D.; Wesdemiotis, C. Dissociation of the Peptide Bond in Protonated Peptides. *J. Mass Spectrom.* **2000,** *35(12),* 1391–1398.
15. Cordero, M. M.; Houser, J. J.; Wesdemiotis, C. The Neutral Products Formed During Backbone Fragmentations of Protonated Peptides in Tandem Mass Spectrometry. *Anal. Chem.* **1993,** *65,* 1594–1601.
16. Nold, M. J.; Wesdemiotis, C.; Yalcin, T.; Harrison, A. G. Amide Bond Dissociation in protonated Peptides. Structures of the N-terminal Ionic and Neutral Fragments. *Int. J. Mass Spectrom. Ion Processes* **1997,** *164,* 137–153.
17. Yalcin, T.; Khouw, C.; Csizmadia, I. G.; Peterson, M. R.; Harrison, A. G. The Structure and Fragmentation of b_n ($n \geq 3$) Ions in Peptide Spectra. *J. Am. Soc. Mass Spectrom.* **1995,** *6,* 1165–1174.
18. Polfer, N. C.; Oomens, J.; Suhai, S.; Paizs, B. Spectroscopic and Theoretical Evidence for Oxazolone Ring Formation in Collision Induced Dissociation of Peptides. *J. Am. Chem. Soc.* **2005,** *127,* 17154–17155.
19. Polfer, N. C.; Oomens, J.; Suhai, S.; Paizs, B. Infrared Spectroscopy and Theoretical Studies on Gas-Phase Protonated Leu-enkephalin and Its Fragments: Direct Experimental Evidence for the Mobile Proton. *J. Am. Chem. Soc.* **2007,** *129,* 5887–5897.
20. Harrison, A. G.; Young, A. B.; Bleiholder, B.; Suhai, S.; Paizs, B. Scrambling of Sequence Information in Collision-Induced Dissociation of Peptides. *J. Am. Chem. Soc.* **2006,** *128,* 10364–10365.
21. Tang, X-J.; Thibault, P.; Boyd, R. K. Fragmentation Reactions of Multiply-protonated Peptides and Implications for Sequencing by Tandem Mass-spectrometry with Low-Energy Collision-induced Dissociation *Anal. Chem.* **1993,** *65,* 2824–2834.
22. Riba-Garcia, I.; Giles, K.; Bateman, R. H.; Gaskell, S. J. Evidence for Structural Variants of a- and b-Type Peptide Fragment Ions Using Combined Ion Mobility/Mass Spectrometry. *J. Am. Soc. Mass Spectrom.* **2008,** *19,* 609–613.
23. Farrugia, J. M.; O'Hair, R. A. J.; Reid, G. E. Do All b_2 Ions Have Oxazolone Structures? Multistage Mass Spectrometry and Ab Initio Studies on Protonated *N*-Acyl Amino Acid Methyl Ester Model Systems. *Int. J. Mass Spectrom. Ion Processes* **2001,** *210/211,* 71–87.
24. Gu, C.; Tsaprailis, G.; Breci, L.; Wysocki, V. H. Selective Gas-Phase Cleavage at the Peptide Bond C-Terminal to Aspartic Acid in Fixed-Charge Derivatives of Asp-Containing Peptides. *Anal. Chem.* **2000,** *72,* 5804–5813.
25. Tsaprailis, G.; Nair, H.; Somogyi, A.; Wysocki, V. H.; Zhong, W.; Futrell, J. H.; Summerfield, S. G.; Gaskell, S. J. Influence of Secondary Structure on the Fragmentation of Protonated Peptides. *J. Am. Chem. Soc.* **1999,** *121,* 5142–5154.
26. Farrugia, J. M.; Taverner, T.; O'Hair, R. A. J. Side-Chain Involvement in the Fragmentation Reactions of the Protonated Methyl Esters of Histidine and Its Peptides. ***2001,*** *209,* 99–112.
27. Savitski, M. M., Falth, M., Eva Fung, Y. M., Adams, C. M., Zubarev, R. A., Bifurcating Fragmentation Behavior of Gas-Phase Tryptic Peptide Dications in Collisional Activation. *J. Am. Soc. for Mass Spectrom.* (2008), doi. 10.1016/j.jasms.2008.08.003.
28. Vachet R. W; Ray K. L.; Glish, G. L. Origin of Product Ions in the MS/MS Spectra of Peptides in a Quadrupole Ion Trap. *J. Am. Soc. Mass Spectrom.* **1998,** *9,* 341–344.
29. Paizs, B.; Szlavik, Z.; Lendvay, G.; Vékey, K.; Suhai, S. Formation of a_2^+ ions of protonated peptides. An Ab Initio Study. *Rapid Commun. Mass Spectrom.* **2000,** *14,* 746–755.
30. Vachet, R. W.; Bishop, B. M.; Erickson, B. W.; Glish, G. L. Novel Peptide Dissociation: Gas-Phase Intramolecular Rearrangement of Internal Amino Acid Residues. *J. Am. Chem. Soc.* **1997,** *119,* 5481–5488.
31. Polfer, N. C.; Bohrer, B. C.; Plasencia, M. D.; Paizs, B.; Clemmer, D. E. On the Dynamics of Fragment Isomerization in Collision-Induced Dissociation of Peptides. *J. Phys. Chem. A* **2008,** *112,* 1286–1293.
32. Bleiholder, C.; Osburn, S.; Williams, T. D.; Suhai, S.; Van Stipdonk, M.; Harrison, A. G.; Paizs, B. Sequence Scrambling Fragmentation Pathways of Protonated Peptides, unpublished.
33. *Fmoc Solid Phase Peptide Synthesis—A Practical Approach*; Chan, W. C.; White, P. D.; Eds; Oxford University Press: New York, 2000.
34. Barr, J. M.; Van Stipdonk, M. J. Multi-Stage Tandem Mass Spectrometry of Metal Cationized Leucine Enkephalin and Leucine Enkephalin Amide. *Rapid Commun. Mass Spectrom.* **2002,** *16,* 566–578.
35. Paizs, B.; Suhai, S. Combined Quantum Chemical and RRKM Modeling of the Main Fragmentation Pathways of Protonated GGG. II. Formation of b_2, y_1, and y_2 ions. *Rapid Commun. Mass Spectrom.* **2002,** *16,* 375–389.
36. Case, D. A.; Pearlman, D. A.; Caldwell, J. W.; Cheatham III, T. E.; Ross, W. S., Simmerling, C. L.; Darden, T. A.; Merz, K., M.; Stanton, R. V.; Cheng, A. L.; Vincent, J. J.; Crowley, M.; Tsui, V.; Radmer, R. J.; Duan, Y.; Pitera, J.; Massova, I. G.; Seibel, G. L.; Singh, U. C.; Weiner, P. K.; Kollmann, P. A. AMBER 99, University of California: San Francisco, **1999**.
37. Gaussian 03, Revision C.02, Frisch, M. J.; Trucks, G. W.; Schlegel, H. B.; Scuseria, G. E.; Robb, M. A.; Cheeseman, J. R.; Montgomery, Jr., J. A.; Vreven, T.; Kudin, K. N.; Burant, J. C.; Millam, J. M.; Iyengar, S. S.; Tomasi, J.; Barone, V.; Mennucci, B.; Cossi, M.; Scalmani, G.; Rega, N.; Petersson, G. A.; Nakatsuji, H.; Hada, M.; Ehara, M.; Toyota, K.; Fukuda, R.; Hasegawa, J.; Ishida, M.; Nakajima, T.; Honda, Y.; Kitao, O.; Nakai, H.; Klene, M.; Li, X.; Knox, J. E.; Hratchian, H. P.; Cross, J. B.; Bakken, V.; Adamo, C.; Jaramillo, J.; Gomperts, R.; Stratmann, R. E.; Yazyev, O.; Austin, A. J.; Cammi, R.; Pomelli, C.; Ochterski, J. W.; Ayala, P. Y.; Morokuma, K.; Voth, G. A.; Salvador, P.; Dannenberg, J. J.; Zakrzewski, V. G.; Dapprich, S.; Daniels, A. D.; Strain, M. C.; Farkas, O.; Malick, D. K.; Rabuck, A. D.; Raghavachari, K.; Foresman, J. B.; Ortiz, J. V.; Cui, Q.; Baboul, A. G.; Clifford, S.; Cioslowski, J.; Stefanov, B. B.; Liu, G.; Liashenko, A.; Piskorz, P.; Komaromi, I.; Martin, R. L.; Fox, D. J.; Keith, T.; Al-Laham, M. A.; Peng, C. Y.; Nanayakkara, A.; Challacombe, M.; Gill, P. M. W.; Johnson, B.; Chen, W.; Wong, M. W.; Gonzalez, C.; and Pople, J. A.; Gaussian, Inc., Wallingford CT, **2004**.
38. Harrison, A. G.; Young, A. B. Fragmentation of Protonated Oligoalanines: Amide Bond Cleavage and Beyond. *J. Am. Soc. Mass Spectrom.* **2004,** *15,* 1810–1819.
39. Cooper, T.; Talaty, E.; Grove, J.; Suhai, S.; Paizs, B.; Van Stipdonk, M. Isotope Labeling and Theoretical Study of the Formation of a_3* Ions from Protonated Tetraglycine. *J. Am. Soc. Mass Spectrom.* **2006,** *17,* 1654–1664.
40. Bythell, B. J.; Barofsky, D. F., Pingitore, F.; Wang, P., Wesdemiotis, C.; Paizs, B. Backbone Cleavages and Sequential Loss of Carbon Monoxide and Ammonia from Protonated AGG: A Combined Tandem Mass Spectrometry, Isotope Labeling, and Theoretical Study. *J. Am. Soc. Mass Spectrom.* **2007,** *18,* 1291–1303.
41. Kinser, R. D.; Ridge, D. P.; Hvistendahl, G.; Rasmussen, B.; Uggerud, E. The Unimolecular Chemistry of Protonated Glycinamide and the Proton Affinity of Glycinamide Mass Spectrometric Experiments and Theoretical Model. *Chem. Eur. J.* **1996,** *2,* 1143–1149.
42. Allen, J. M.; Black, D. M.; Johnson, J. S.; Glish, G. L.; Bythell, B. J.; Paizs, B. Why Do b3 Ions not Form a3 Ions? Unpublished.